LASER INTERFEROMETER GRAVITATIONAL WAVE OBSERVATORY

LIGO Laboratory / LIGO Scientific Collaboration

LIGO- T1200425-v1 *LIGO* 08/30/12

Wide Angle Scatter from ETM HR

Michael Smith

Distribution of this document:
LIGO Scientific Collaboration

This is an internal working note
of the LIGO Laboratory.

California Institute of Technology
LIGO Project – MS 18-34
1200 E. California Blvd.
Pasadena, CA 91125
Phone (626) 395-2129
Fax (626) 304-9834
E-mail: info@ligo.caltech.edu

Massachusetts Institute of Technology
LIGO Project – NW22-295
185 Albany St
Cambridge, MA 02139
Phone (617) 253-4824
Fax (617) 253-7014
E-mail: info@ligo.mit.edu

LIGO Hanford Observatory
P.O. Box 159
Richland WA 99352
Phone 509-372-8106
Fax 509-372-8137

LIGO Livingston Observatory
P.O. Box 940
Livingston, LA 70754
Phone 225-686-3100
Fax 225-686-7189

http://www.ligo.caltech.edu/

Table of Contents

Table of Tables

Table of Figures

Abstract:

The displacement noise, m/rtHz @ 100 Hz, caused by re-scattering of wide-angle scattered light from the H1 ETMX was determined by using the ZEMAX ray trace detector and the scattering cross-section reciprocity theorem of Flanagan-Thorne; the displacement noise meets the SLC requirement.

1 INTRODUCTION

Defects or dust on the test mass (TM) cavity mirrors scatter power into wide angles $0.1 < \theta < \pi/2$; see T070089-02, Wide Angle Scatter from LIGO Arm Cavities. The angular scatter distribution is presumed to be Lambertian (i.e. "flat"), such that the probability of a cavity photon scattering to angle θ off axis is given by $B_L = \frac{\alpha \cos\theta}{\pi}$ where α is a constant, nominally the "Lambertian reflectance." This is reasonable for small point defects, and approximately consistent with Kells' measurements out to $\theta \approx \pi/4$. The value for α has been estimated by Hiro Yamamoto in G070240 to be 10 ppm of loss for wide-angle (point-defect) scatter.

The wide angle scattering from the H1 ETMX HR surface was analyzed using ZEMAX ray tracing by applying a Lambertian scattering property to the TM HR surface and detecting the scattered light with detector surfaces. More than 75% of the wide-angle scattered light from the ETM HR surface will be captured by the ACB and wide angle box. 4% passes through the hole in the arm cavity baffle and will hit the 7A2 spool piece or the support structure for the Photon Calibrator mirrors; the remaining rays hit the TM SUS structure and the walls of the BSC chamber.

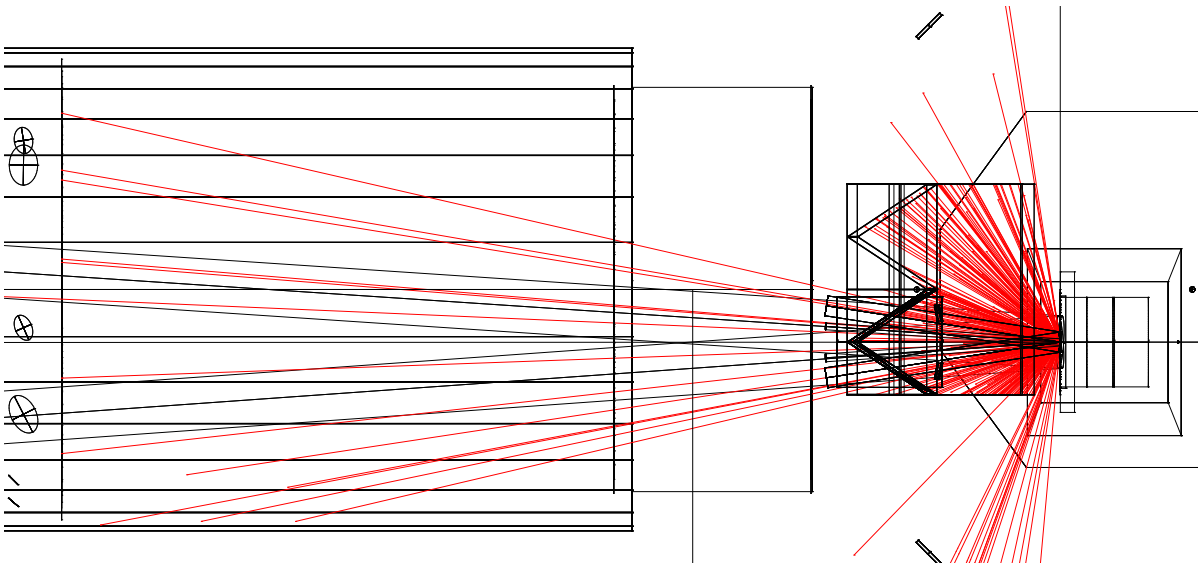

Figure 1: ZEMAX Lambertian Scatter Ray Trace from H1 ETMX HR Hitting ACB with Wide Angle Baffle Box, Top View

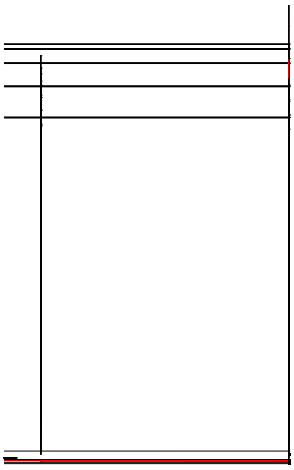

Figure 2: ZEMAX Lambertian Scatter Ray Trace from H1 ETMX HR, Hitting ACB with Wide Angle Baffle Box, Side View

2 SCATTERED LIGHT NOISE THEORY

The wide angle scattered light from the TM that hits an adjacent surface will scatter from that surface back onto the TM and then re-scatter from the TM into the mode of the interferometer (IFO).

The fraction of the arm power incident on the TM Lambertian scattering surface that scatters at wide angles onto each adjacent surface near the TM can be calculated in principle by knowing the Lambertian scatter function of the TM and the scattering geometry.

Lambertian scatter function for the TM

$$BRDF_L := \alpha_L \cdot \frac{\cos(\theta)}{\pi}$$

differential wide angle scattered light from TM onto adjacent surfaces

$$dP_{sadj} := P_a \cdot BRDF_L \cdot d\Omega$$

total wide angle scattered light from TM onto adjacent surfaces

$$P_{sadj} := P_a \cdot \alpha_L \cdot \int_{\theta_{s1}}^{\theta_{s2}} \frac{\cos(\theta)}{\pi} \, d\Omega$$

However, the geometry is complex, and it is more convenient to use the ZEMAX ray detector program for determining the incident power that hits each adjacent surface. The ZEMAX power fraction is defined as follows:

ZEMAX power fraction

$$PF_s := \int_{\theta_{s1}}^{\theta_{s2}} \frac{\cos(\theta)}{\pi} \, d\Omega$$

incident power hitting the adjacent surface is

$$P_{inc} := P_a \cdot \alpha_L \cdot PF_s$$

The adjacent surface is located a distance Ls away. The back-scattered power from the surface with a BRDFs will irradiate the TM.

irradiance of TM by power scattered from adjacent surface, W/m^2

$$E_s := P_{inc} \cdot BRDF_s \cdot \frac{1}{L_s^2}$$

Some of this irradiance will be scattered by the TM back into the IFO mode. To determine the fraction that is recombined into the cavity mode, we rely on a reciprocity relation derived by E. Flanagan and K. Thorne in LIGO Technical note T940063-00-R. They calculate the cross section, $\sigma(z, \vec{y})$, for a cavity mirror to scatter photons arriving from a point $(z, \vec{y})$ back into the cavity mode ($\vec{y}$ is a location in the plane z = constant a distance z from the mirror along the optic axis). They find this cross section is related to the probability $dP / d\Omega(z, \vec{y})$ for the cavity mirror to scatter photons out of the main beam to the point $(z, \vec{y})$:

$$\sigma(z, \vec{y}) = \lambda^2 \frac{dP(z, \vec{y})}{d\Omega}.$$

In this case, the probability $dP / d\Omega(z, \vec{y})$ is the Lambertian BRDF function, written above.

According to their reciprocity theorem, the power scattered back into the IFO mode from each adjacent surface is given by

$$P_{sifo} := E_s \cdot \sigma$$

where Es is the irradiance, W/m^2, of the cavity mirror by that adjacent surface. Then,

$$P_{sifo} := P_{inc} \cdot BRDF_s \cdot \frac{\lambda^2}{L_s^2} \cdot \alpha_L \cdot \frac{\cos(\theta_{inc})}{\pi}$$

Flanagan-Thorne calculate the displacement noise caused by this injected scattered field fluctuation in the arm cavity.

$$DN_{s\_thorne} := \left(\frac{P_{sifo}}{P_a}\right)^{0.5} \cdot \frac{\lambda}{4 \cdot \pi \cdot L} \cdot S \cdot L$$

Where S is the amplitude spectral density of sine phase fluctuations of the injected field

$$S := \sqrt{8 \cdot \pi^2 \cdot \frac{x_s^2}{\lambda^2}}$$

In the formalism of Smith and Yamamoto, the displacement noise, in m/rtHz, caused by the scattered field injected into the IFO mode is proportional to the DARM transfer function (see T060073), to the square root of the scattered power relative to the PSL power, and to the seismic motion amplitude spectrum of the scattering surface.

$$DN_{s\_smith} := TF_{itmhr} \cdot \left(\frac{P_{sifo}}{P_{psl}}\right)^{0.5} \cdot \frac{2 \cdot k \cdot x_s}{\sqrt{2}}$$

Where the factor rt2, following Flanagan-Thorne, corrects for the slow phase motion that is below the gravity wave frequency band.

These two apparently different approaches agree to within < 5%.

3 RESULTS OF WIDE ANGLE SCATTER NOISE CALCULATIONS

3.1 Wide Angle Scattered Light Calculation Parameters

Displacement noise requirement @ 100 Hz, m/rt Hz	$D_{req} := 1 \cdot 10^{-21}$
Motion of manifold @ 100 Hz, m/rt Hz	$x_{manifold} := 8 \cdot 10^{-11}$
ACB displacement @ 100 Hz, m/rtHz	$x_{ACB} := 1 \cdot 10^{-12}$
ISI optical table displacement @ 100 Hz, m/rtHz	$x_{ISI} := 3 \cdot 10^{-14}$
Transfer function @ 100 Hz, ITM HR	$TF_{itmhr} := 1.1 \cdot 10^{-9}$
BRDF of chamber wall, sr^-1	$BRDF_{wall} := 0.1$
BRDF of oxidized un-polished steel, sr^-1	$BRDF_{oxiunpolish} := 0.03$
laser wavelength, m	$\lambda := 1.064 \cdot 10^{-6}$
wave number, m^-1	$k := 2 \cdot \frac{\pi}{\lambda}$ $k = 5.905 \times 10^{6}$
wide angle hemispherical scattering loss fraction from TM wide, ref: T070089	$\alpha_L := 10 \times 10^{-6}$
arm power, W	$P_a := 8.125 \times 10^{5}$
input laser power, W	$P_{psl} := 125$
arm cavity length, m	$L := 4000$

3.2 Scattered Light Results

Table 1 summarizes the results of the ZEMAX measurements of the fractional wide angle scatter from the ETM onto each adjacent scattering surface.

Table 1: Wide Angle Scattered Light Power distribution from H1 ETMX, Determined Using ZEMAX Ray Detector

Surface	Power, W	fractional scatter	scattering length, mm	incident angle, deg	incident angle, rad
Annular Volume 1080: spool 7A2 large dia	1.22	0.01	7446	5.5	0.10
PCal structure	2.78	0.03	2371	5	0.09
BSC bottom	3.11	0.03	2248	103	1.80
BSC right	5.44	0.05	1566	105	1.83
BSC left	0.44	0.004	1967	99	1.73
ITM/ETM middle envelope	4.56	0.05	172	103	1.81
ARM CAVITY BAF PLATE top ETMX	0.44	0.00	764	57	0.99
ARM CAVITY BAF PLATE BOTTOM ETMX	2.78	0.03	572	39	0.67
ARM CAVITY BAF PLATE 2 ETMX	6.89	0.07	716	47	0.82
ARM CAVITY BAF PLATE 3 ETMX	2.11	0.02	605	35	0.61
ARM CAVITY BAF PLATE 4 ETMX	0.89	0.01	468	26	
ARM CAVITY BAF PLATE 5 ETMX	5.78	0.06	475	19	0.34
ARM CAVITY BAF PLATE 6 ETMX	6.33	0.06	443	18	0.31
ARM CAVITY BAF PLATE 7 ETMX	0.78	0.01	231	9	0.15
WIDE ANGLE BAF TOP LEDGE ETMX	7.22	0.07	901	41	0.71
WIDE ANGLE BAF BOTTOM LEDGE ETMX	21.89	0.22	748	29	0.51
acb_wide-angle-baffle-side_H1_ITMx.POB Right	19.22	0.19	895	31	0.54
acb_wide-angle-baffle-side_H1_ITMx.POB Left	5.67	0.06	788	26	0.46

Table 2 summarizes the calculated incident powers and the powers scattered into the IFO mode.

Table 2: Wide Angle Scattered Light Power Back into IFO Mode

Surface	Incident Power, W	Power Scattered into IFO, W	BRDF, sr^-1	Motion Spectrum
Annular Volume 1080: spool 7A2 large dia	0.099	1.28E-21	0.1	MANIFOLD
Detector Surface 1084: PCal structure	0.226	2.88E-20	0.1	MANIFOLD
Detector Surface 1118: BSC bottom	0.253	2.26E-20	0.1	BSC
Detector Surface 1119: BSC front	0.442	6.23E-22	0.1	BSC

Surface	Incident Power, W	Power Scattered into IFO, W	BRDF, sr^-1	Motion Spectrum
Detector Surface 1120: BSC back	0.036	2.59E-21	0.1	BSC
Rectangular Volume 1115: ITM/ETM middle envelope	0.370	6.42E-19	0.05	ISI
Rectangular Volume 1127: ARM CAVITY BAF PLATE top ETMX	0.036	7.33E-21	0.05	ACB SUS
Rectangular Volume 1128: ARM CAVITY BAF PLATE BOTTOM ETMX	0.226	1.17E-19	0.05	ACB SUS
Rectangular Volume 1130: ARM CAVITY BAF PLATE 2 ETMX	0.560	1.78E-19	0.05	ACB SUS
Rectangular Volume 1131: ARM CAVITY BAF PLATE 3 ETMX	0.171	8.33E-20	0.05	ACB SUS
Rectangular Volume 1132: ARM CAVITY BAF PLATE 4 ETMX	0.072	6.36E-20	0.05	ACB SUS
Rectangular Volume 1133: ARM CAVITY BAF PLATE 5 ETMX	0.470	4.00E-19	0.05	ACB SUS
Rectangular Volume 1147: ARM CAVITY BAF PLATE 6 ETMX	0.514	5.12E-19	0.05	ACB SUS
Rectangular Volume 1161: ARM CAVITY BAF PLATE 7 ETMX	0.063	2.49E-19	0.05	ACB SUS
Rectangular Volume 1163: WIDE ANGLE BAF TOP LEDGE ETMX	0.587	9.70E-20	0.05	ACB SUS
Rectangular Volume 1164: WIDE ANGLE BAF BOTTOM LEDGE ETMX	1.779	5.04E-19	0.05	ACB SUS
Polygon Object 1165: acb_wide-angle-baffle-side_H1_ITMx.POB Right	1.560	2.63E-19	0.05	ACB SUS
Polygon Object 1166: acb_wide-angle-baffle-side_H1_ITMx.POB Left	0.461	1.13E-19	0.05	ACB SUS

Table 3 summarizes the displacement noise, m/rtHz @ 100 Hz, caused by re-scattering of wide-angle scattered light from the ETM by each of the major surface groupings.

Table 3: Displacement Noise caused by Re-scattering of Wide Angle Scattered Light from ETM

Surface	Displacement Noise @ 100 Hz, m/rtHz
spool 7A2	2.35E-24
PCal structure	1.12E-23
BSC chamber walls	9.91E-24
ITM/ETM SUS structure	1.97E-26
ARM CAVITY BAF	7.97E-25

The displacement noise spectra caused by re-scattering of the wide angle scattered light from the ETM are shown in Figure 3; the noise meets the SLC requirement.

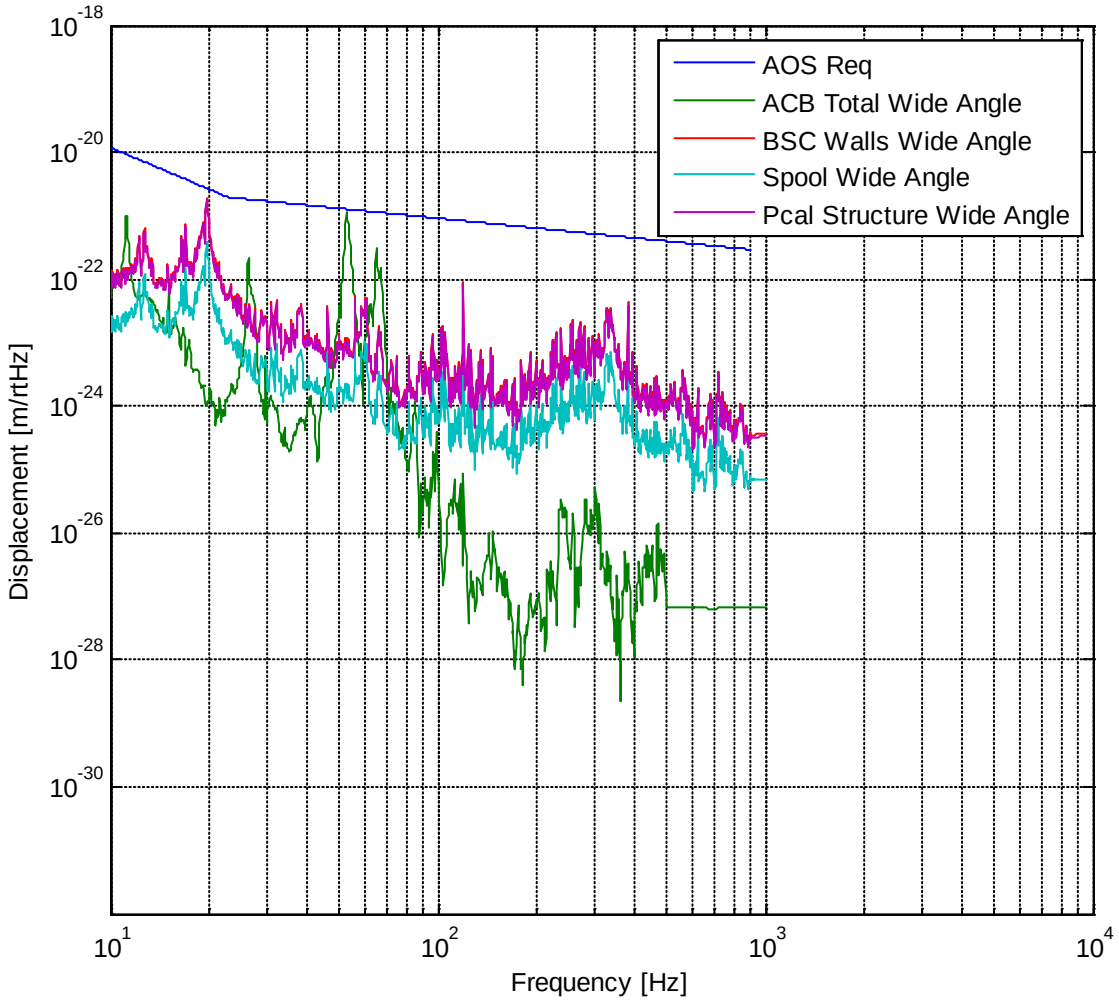

Figure 3: Displacement Noise from Wide Angle Scattering by ETM